Click here to view PowerPoint presentation; Press Esc to exit

Effect of Side Jets in a Supersonic Flow Measured and Calculated on a Flat Plate and a Generic Missile Configuration

Anke Kovar, Erich Schülein
German Aerospace Center, DLR Germany
Institute for Aerodynamics and Flow Technology
Bunsenstr. 10
37073 Göttingen
GERMANY

Anke.Kovar@dlr.de, Erich.Schuelein@dlr.de

ABSTRACT

An investigation on side jets in an M = 5.0 flow was conducted on a flat plate as well as on a generic missile configuration. Surface pressure measurements, oil flow visualisations, force measurements and associated numerical simulations gave insight into the interaction of different jet configurations and their influence on the efficiency of side jet control described by the amplification factor. The analysis of the data especially in the wake of the jet showed that the low pressure region is much less dominant than assumed and that the position of the side jet nozzle is vital also with respect to the exploitation of a desired amplification of the side jet thrust.

1.0 INTRODUCTION

Jets exhausting into a supersonic flow are a well-known tool to control highly agile missiles. Its advantages are the very quick response of only milliseconds and its applicability also at low dynamic pressures, e.g. high altitudes or starting phase, where conventional control surfaces become ineffective. The drawback is the difficult predictability of the interaction of the side jet control with the oncoming flow and the boundary layer that is developing along the fuselage, and its strong dependence on flight parameters like stagnation pressure, making the effect uncertain.

The interaction is causing a three-dimensional, complex, and unsteady flow field, as the issuing jet is acting as a fluctuating obstacle in the main flow (Figure 1). Consequently, a bow shock is developing ahead of the jet front. Upstream of the jet, the boundary layer of the fuselage experiences a pressure rise and finally separates. An oblique separation shock develops above this area. Between the primary separation line and the reattachment line upstream of the jet, a horseshoe vortex is created and transports boundary layer material downstream. In the wake of the jet, a rear separation zone occurs. In this area, where the jet blocks the main flow, low pressures are measured. Where the flow reattaches, the pressure increases with a recompression shock to the nearly undisturbed value upstream of the interaction.

The efficiency of the side jet control depends strongly on the size and position of the separation zones, due to the herewith related pressure levels in the high pressure region as well as in the wake of the jet. This is described by the so-called amplification factor K_F, which relates the force due to the interaction of the jet with the flow (so-called interaction force) F_i with the force due to the available energy of the jet (so-called jet force) F_j

$$K_F = \frac{F_j + F_i}{F_j}. \qquad (1)$$

Kovar, A.; Schülein, E. (2006) Effect of Side Jets in a Supersonic Flow Measured and Calculated on a Flat Plate and a Generic Missile Configuration. In *Innovative Missile Systems* (pp. 37-1 – 37-16). Meeting Proceedings RTO-MP-AVT-135, Paper 37. Neuilly-sur-Seine, France: RTO. Available from: http://www.rto.nato.int/abstracts.asp.

Report Documentation Page

Form Approved
OMB No. 0704-0188

Public reporting burden for the collection of information is estimated to average 1 hour per response, including the time for reviewing instructions, searching existing data sources, gathering and maintaining the data needed, and completing and reviewing the collection of information. Send comments regarding this burden estimate or any other aspect of this collection of information, including suggestions for reducing this burden, to Washington Headquarters Services, Directorate for Information Operations and Reports, 1215 Jefferson Davis Highway, Suite 1204, Arlington VA 22202-4302. Respondents should be aware that notwithstanding any other provision of law, no person shall be subject to a penalty for failing to comply with a collection of information if it does not display a currently valid OMB control number.

1. REPORT DATE	2. REPORT TYPE	3. DATES COVERED
01 MAY 2006	**N/A**	**-**

4. TITLE AND SUBTITLE	5a. CONTRACT NUMBER
Effect of Side Jets in a Supersonic Flow Measured and Calculated on a Flat Plate and a Generic Missile Configuration (U)	5b. GRANT NUMBER
	5c. PROGRAM ELEMENT NUMBER
6. AUTHOR(S)	5d. PROJECT NUMBER
	5e. TASK NUMBER
	5f. WORK UNIT NUMBER
7. PERFORMING ORGANIZATION NAME(S) AND ADDRESS(ES) **German Aerospace Center, DLR Germany Institute for Aerodynamics and Flow Technology Bunsenstr. 10 37073 Göttingen GERMANY**	8. PERFORMING ORGANIZATION REPORT NUMBER
9. SPONSORING/MONITORING AGENCY NAME(S) AND ADDRESS(ES)	10. SPONSOR/MONITOR'S ACRONYM(S)
	11. SPONSOR/MONITOR'S REPORT NUMBER(S)

12. DISTRIBUTION/AVAILABILITY STATEMENT
Approved for public release, distribution unlimited

13. SUPPLEMENTARY NOTES
See also ADM401233. RTO-MP-AVT-135, Presented at the RTO Applied Vehicle Technology Panel (AVT) Business Meeting Week in Amsterdam, the Netherlands, 15-18 May 2006., The original document contains color images.

14. ABSTRACT
See the report.

15. SUBJECT TERMS

16. SECURITY CLASSIFICATION OF:			17. LIMITATION OF ABSTRACT	18. NUMBER OF PAGES	19a. NAME OF RESPONSIBLE PERSON
a. REPORT	b. ABSTRACT	c. THIS PAGE			
unclassified - NATO	**unclassified**	**unclassified**	**SAR**	**33**	

Standard Form 298 (Rev. 8-98)
Prescribed by ANSI Std Z39-18

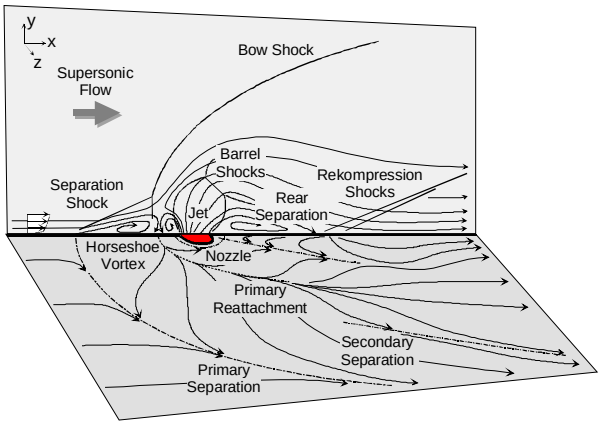

Figure 1: Schematic representation of the general flow field developing due to the side jet interaction.

If K_F exceeds 1, there is a gain additionally to the thrust of the jet itself resulting from the interaction of the side jet with the flow, if it is smaller than 1, the jet thrust is alleviated. The investigation shows that the problem is very complex. If the separation zone becomes too big, it might embrace the whole missile body, reducing the effect of the interaction area. Thus, the target of the investigation has to be the finding of a configuration that is effective, but more than that, it has to be stable for the greater the range of angles of attack, the better. For this reason, a study was conducted that encompassed different jet configurations to see whether the interaction can be stabilised and also be predicted by the applied TAU-code. The investigations started off with experiments on the flat plate, as many of the general flow features can be seen more easily but for application purposes it was essential to investigate the effects also on a generic missile configuration.

2.0 SIDE JETS ON A FLAT PLATE

2.1 Experimental setup of the flat plate

The experiments were conducted in the super- and hypersonic Ludwieg Tube (RWG) at DLR. The Ludwieg Tube consists of an 80 m long storage tube which is separated from the measurement section and a vacuum tank by a fast responding gate valve. If the gate valve is opened, quasi-constant conditions are measured in the measurement section for about 300 – 350 ms. The tunnel covers a Mach number range of $3 \leq M \leq 7$ and Reynolds numbers between $5 \cdot 10^6 \leq Re \leq 60 \cdot 10$ m^{-1}. The test conditions for this study on the flat plate were chosen with $M_\infty = 5.0$ and $Re_\infty = 38 \cdot 10^6$ m^{-1} which produced turbulent conditions in the interaction region. The test section for this Mach number has got a circular cross section of 0.5 m. Further details can be found in [6] and [10].

The investigation was conducted on two different models, a flat plate, which is described in the following and a generic missile described in chapter 3.1 following. On the flat plate surface pressure measurements and oil flow visualisations were conducted. The dimension of the flat plate was 660 mm in length (x-direction) and 400 mm in width (z-direction). 360 mm downstream of the leading edge, a sonic nozzle was mounted in the centreline of the model with a diameter of 6 mm out of which a jet was issued (Figure 2). In further experiments the single nozzle was replaced by four nozzles, mounted in-line or side-by-side. The cross-sectional area of the single nozzle was kept constant for the four nozzle-cases, as the focus was on the investigation of the influence of different configurations rather than different pressure ratios. The surface pressure measurements were carried out with PSI modules. 160 pressure taps were distributed over

the surface on half around the side jet, assuming symmetry of the flow, with an inner diameter of the taps of 0.3 mm. Those pressure measurements were later on taken for the comparison of the surface pressure with the numerical calculations.

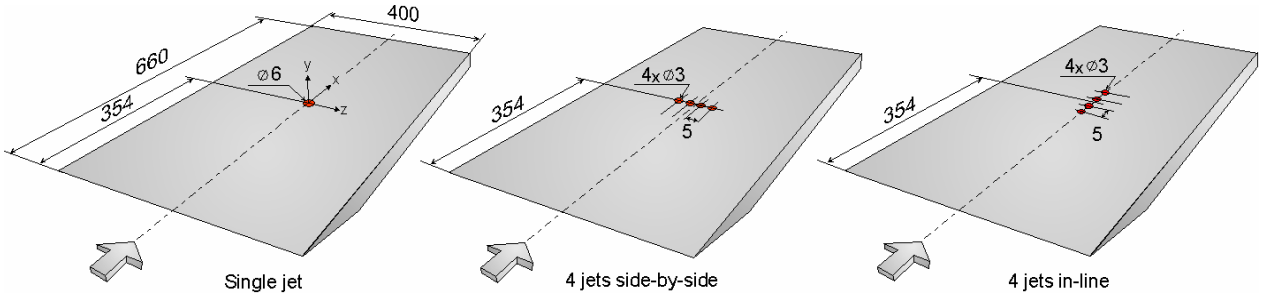

Figure 2: Schematic representation of the flat plate model for the single jet, four side-by-side jets and in-line.

The jet pressure ratio (total jet pressure p_{0jet} over free-stream static pressure in the wind tunnel p_∞) for the investigations on the flat plate was adjusted to a value of $p_{0jet}/p_\infty = 100$ and controlled via total pressure measurements in the nozzle inlet.

2.2 Numerical studies of the flat plate

The numerical studies were performed with the DLR-internal developed TAU-code. For further reference see [3] and [11]. It is an unstructured Reynolds-averaged Navier-Stokes-solver for compressible flows with a variety of different 1- and 2-equation turbulence models. The calculations here have been conducted with the 1-eqn. model by Spalart-Almaras with Edwards-modification. The required grids were generated with the commercial hybrid grid generator Centaur™. The grids were generated with a y+ of about 1 in the first cell height, which is an important criterion for a proper turbulence modelling. Deviations from that were corrected during the process of calculation with the automatic adaptation tool. The grid cells were refined already in the initial grid in areas were large gradients are expected, e.g. around the jet. The grids were further refined by automatic adaptation, where threshold values of density, velocity, total pressure and enthalpy were observed. The numerical calculations were continued for each case as long as gradients above these threshold values occurred and the main coefficients like drag and lift were still changing. When they reached an asymptotic value, the residual did fall by some orders of magnitude, and the observed parameters like surface pressure and separation lines ceased to change, the solution of the calculation was considered to be converged. The grid consisted of a structured part resolving the boundary layer. The stretching factor in the initial grids for the flat plate cases was set to 1.28, and the number of prismatic layers resolving the boundary layer was set to 25. The procedure for the grid generation and setup as well as the grid studies is described more detailed in [5].

As the averaged flow phenomenon appears to be very complex but still symmetric to the middle axis concerning the flow features, it was decided to calculate with a symmetry plane. The symmetry plane is finally forcing symmetry of the flow features along the middle axis that is halfway cutting through the nozzle, but it has the advantage of saving grid points and herewith calculation time. The side jet control was simplified for either case, flat plate and full body configuration, in comparison to the experiment. The jet flow was realised through a circular area which was set as a supersonic inflow instead of going through a reservoir and a nozzle. With this boundary condition it was possible to issue a jet similar to through a sonic nozzle, which means that the issuing jet was blowing out of this circular area with a diameter of 6 mm at a Mach number of $M = 1.0$ with then total jet pressure as in the wind tunnel experiments. Still, it is likely that the mass flow through this area was not the same as in the experiment, as in reality a boundary

layer or friction effects are evolving along the rim of the jet nozzle and are reducing the effective cross sectional area out of which the jet is being issued.

The flow Mach number was also chosen with M = 5.0, whereas the jet pressure ratio p_{0jet}/p_{∞} was set to 100 for the case of the flat plate, as in the experiment.

2.3 Results of the studies on the flat plate

Major investigations were conducted on the flat plate, as the general flow features are the same as they occur on the full body configuration, but the measurements can be conducted more easily and to a greater extent. For three different configurations, the surface pressure was measured in a cut along the middle axis and 3 cuts perpendicular to it to compare the general agreement between numerical simulation and experiment (Figure 3).

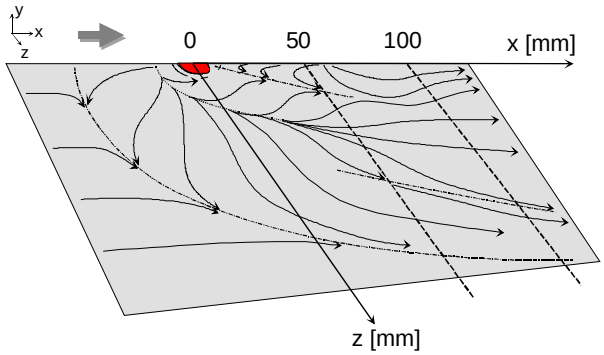

Figure 3: Schematic representation of the four pressure measurement cuts at *z*=0 mm (symmetry plane), *x*=0 mm, *x*=50 mm and *x*=100 mm.

Firstly, wall pressure measurements were conducted for the reference case of a single jet. This is shown in Figure 4a, b, c, and d, which display the direct comparison between experiment and numerical simulation for the four cuts.

The overall agreement of the comparison of the surface pressure is fair; the further downstream the better the agreement of the calculation with the experiment. Figure 4a shows that the separation zone is enlarged in the numerical calculation, shifting the pressure peaks of the plateau as well as of the reattachment line slightly upstream. From Figure 4b it can be seen that the lateral extent of the separation zone for this case with a jet pressure ratio of 100 is more than 40 mm. Transferred to a full body configuration with a diameter of only 30 mm, it becomes clear that this pressure ratio would be too high for the chosen experimental full body configuration as the separation zone would be embracing the whole body.

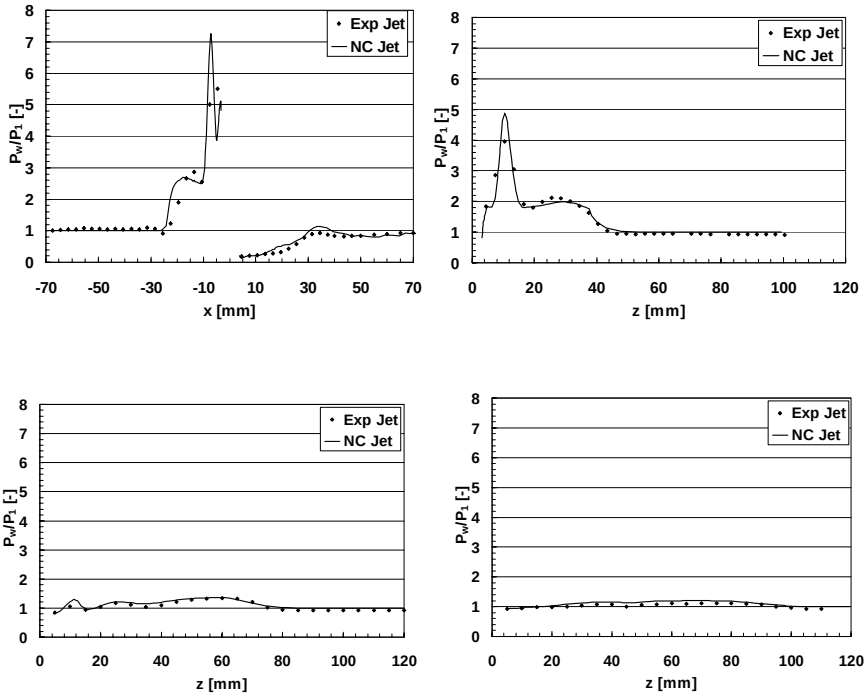

Figure 4a, b, c, and d: Comparison of the surface pressure for the cuts at *z*=0 mm (along the symmetry plane, upper left), *x*=0 (upper right), 50 (lower left), and 100 mm (lower right) for the case of the single jet.

The target of the study was the investigation of the influence different jet configurations might have on the efficiency of the side jet control. For this purpose, the single nozzle was replaced by four nozzles mounted side-by-side (Figure 5b) and in-line (Figure 5c). As mentioned before in the introduction, the cross-sectional area was kept constant for the four nozzle cases in comparison to the single nozzle. To gain deeper insight into the more complex flow behaviour, oil flow visualisations were carried out on the surface of the flat plate. In Figure 5a-c the wall streamlines gained in the experiments (upper half) were compared with the numerical simulations (lower half). It can be seen that the different configurations do have a strong influence on the flow field around the jet(s).

Figure 5a shows the reference case of the single nozzle. Figure 5b shows that four nozzles mounted side-by-side do enlarge the separation zone and create in stream-wise direction as well as lateral to the main flow the greatest separation zone where high pressure will be found. This can be seen on the primary separation line indicated with S. This wider separation zone is provoked by the lateral extent of the four nozzles, blocking the main flow over a wider distance.

On Figure 5c it can be seen that the four jets mounted in-line allow the main flow to by-pass the four nozzles in a closer distance around the nozzles. As the four nozzles have the same nominal cross-sectional area as the single nozzle, but are distributed in flow-direction, they herewith also distribute the jet force longitudinally and this is resulting in a smaller separation zone upstream of the four jets. In general it can be said that the overall agreement between experiment and numerical simulation also here is fair. The separation zone of the numerical calculation is overestimated, more for the single jet and the four jets side-by-side, only very little for the four jets mounted in-line. It seems to be clear that these configurations do have an influence on the efficiency of the side jet control and for the purpose of analysing this effect, a set of different configurations including the cases four nozzles side-by-side and in-line were investigated on the full body configuration.

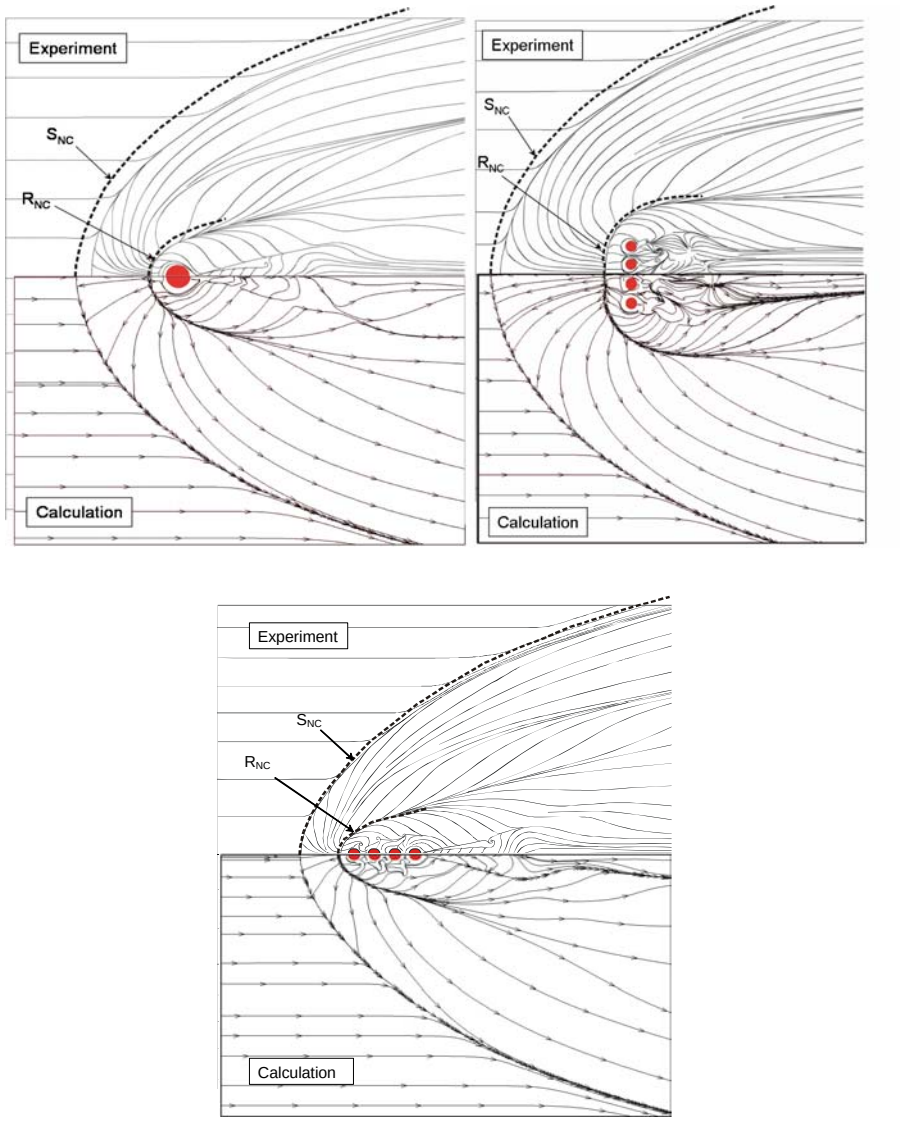

Figure 5a, b, and c: Comparison of wall streamlines for the single jet case (upper left), four jets side-by-side (upper right) and four jets in-line (lower). S and R denote primary separation and reattachment lines. For comparison, the results of the numerical calculations (subscripted with NC) were transferred into the result of the.

Additionally, the numerical simulations enabled the calculation of the amplification factors for the three main configurations of the single jet, four jets in-line and side-by-side. As no force measurements were conducted in the wind tunnel, the results cannot be compared with experiments, only with literature values, where different authors came to a range of results. As the 4 jets mounted in-line and side-by-side act more like 2-dimensional slit nozzles, they are compared with them. [12] found for 2-dimensional slit nozzles mounted perpendicular to the flow direction for Mach numbers between $2.61 < M < 4.54$ and different jet pressure ratios varying between $23.5 < p_{0jet}/p_\infty < 224$ amplification factors of about $2.2 < K_F < 3.2$. A significant dependence on the Mach number was not detected. [7] investigated a slit nozzle covering the whole width of the flat plate model in a Mach number of range of $1.57 < M < 1.83$ and jet pressure ratios of $3 < p_{0jet}/p_\infty < 60$ and gained amplification factors of about $1.8 < K_F < 3.2$. He found that the amplification decreases with increasing jet pressure ratio. [9] found for a single round nozzle of 12.4 mm diameter an amplification of 1.8 at a jet pressure ratio of about 50 and Mach number 4.0. [8] found

amplification factors of $1.9 < K_F < 2.9$ for a single round nozzle of 3.175 mm diameter and jet pressure ratios in a range of $20 < p_{0jet}/p_\infty < 800$. [1] concluded that the induced forces are in general much larger on a flat plate than on a cylinder shaped body like a missile, due to the already described effect that the efficiency is kept in one plane. The results of the investigation discussed in this paper seem to fit well into the range of described literature values.

The determination and analysis of the amplification factor is important for the assessment of jet efficiency. The total amplification factor K_F is given by the integration of the surface pressure. The integration includes the outlet area of the nozzle so that the calculation encompasses the resulting interaction force F_i as well as the force F_j exerted by the jet flow and is divided according to equation 1 in chapter 1.0 by the theoretical jet force F_j given by the potential and kinetic energy of the jet. For the analysis, the pressure was corrected with the surface pressure of the flat plate alone so that only the effect of the interaction is remaining and the integration of the surface pressure was performed along the x- and z-coordinate resulting in an amplification factor in flow direction K_{FX}:

$$K_{FX} = \int_{-x}^{x} \left(\int_{-z}^{z} \Delta p \, dz \right) dx \tag{2}$$

Figure 6 shows the development of the amplification factor along the flat plate K_{FX} for the three cases.

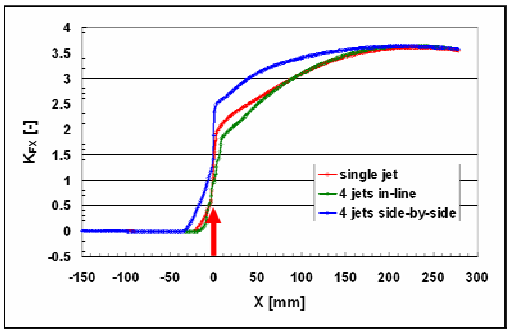

Figure 6: Distribution and development of the calculated amplification factor K_{FX} along the flat plate for single jet, four jets in-line and side-by-side.

There are some interesting, if not unexpected, aspects. Firstly, the amplification factor is not decreasing behind the jet in the region where low pressures exist. Secondly, the amplification factor saturates towards an asymptotic value which is the same for all three different cases.

The first aspect is unanticipated as it was assumed that a low pressure region exists in the wake of the jet where the values are lower than the surface pressure of the undisturbed area upstream of the jet. So it was assumed that substantial parts of the pressure surplus upstream of the jets would be compensated by the low pressure region downstream. In fact, integrating over the whole area where the interaction takes place shows that the horseshoe vortex surrounding the low pressure region is introducing high pressures on the surface so that in the integral of the amplification factor an increase can be seen that progresses through all areas. This can also be seen on the distribution of the surface pressure which is corrected with the surface pressure of a sole flat plate without nozzles so that only the effect of the interaction is visible (Figure 7):

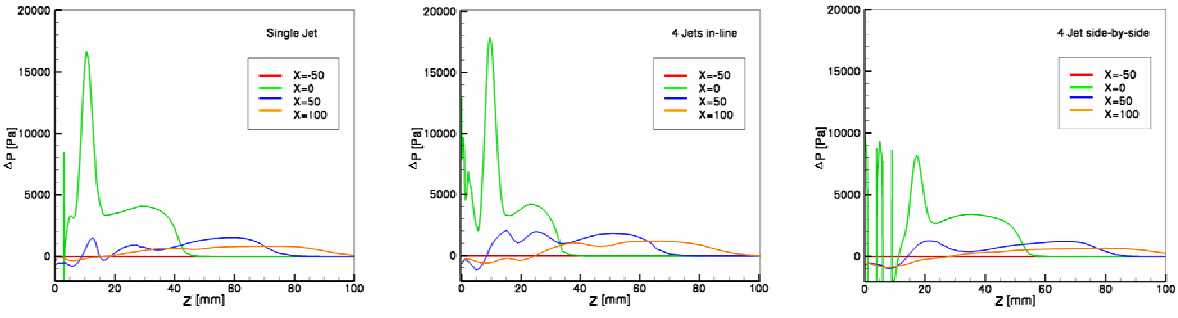

Figure 7: Surface pressure distribution of interaction effect in 4 cuts along the flat plate: x=-50 mm, *x*=0 mm, *x*=50mm, and *x*=100 mm for the three investigated cases.

For x = -50 mm the cut is outside of the interaction area, so only a flat line is visible. For all other curves inside the interaction area it becomes clear that there is only a small area in the wake of the jet(s) where the pressure is below the undisturbed value and the high pressure areas dominate the low pressure regions by far.

The second effect is also unexpected as from the surface pressure distributions and the wall streamlines can be seen that the three different configurations produce separation zones that are different in size and position. Hence, it was concluded that also the amplification factor would be different for the different configurations. From the analysis in Figure 6 can be seen that there is a difference that is vanishing with downstream position and from roughly 280 mm downstream the jet an asymptotic value of K_{FX} of about 3.55 is reached. A direct influence of the configuration type on the amplification factor can only be seen in the vicinity of the jet position. The four jets side-by-side separate earlier than the other two configurations and so is K_{FX} increasing earlier. As also the separation zone of four jets side-by-side is wider than for the other two, K_{FX} increases in the wake of the jets to higher values than the other two cases. Also the behaviour of the single jet and four jets in-line is captured. The single jet configuration has a slightly bigger and wider separation zone upstream of the jet, so the amplification factor increases slightly before for the four jets in-line. In the direct wake the amplification factor is larger for the single jet than for the four jets in-line and with increasing downstream distance K_{FX} of four jets in-line increases disproportionately as the nozzles extend further downstream than the single jet, introducing high pressure through the thrust where the single nozzle is already left behind.

Finally, the amplification factor reaches a value that remains stable for nearly the last 80 mm of the plate. This is also an effect that is induced by the plate itself, as here the flow and the interaction are being kept in this plane. This is in contrast to a full body model where the separation zone embraces and wraps around the body as the normal force vanishes at the sides of the body.

Following from the results, the exact position of the side jet nozzle has to be considered carefully as their position decides about the exploitation of the amplification factor.

3.0 SIDE JETS ON A GENERIC MISSILE CONFIGURATION

3.1 Experimental setup of the generic missile configuration

The second model was a generic missile configuration of 307 mm length and a diameter of 30 mm seen on Figure 8. The special feature of this body was the nose of the configuration which was with a diameter of

5.5 mm opened to the oncoming flow and was used to provide the side jet by redirecting the main flow through the body. As the cross-section of the channel was increasing over its length, it acted as a settling chamber for the flow so that the velocity was very low and the jet was blown out with the total pressure of the flow. The jet pressure ratio for this investigation resulted in p_{0jet}/p_∞ of 32.65 at M = 5.0. The jet diameter was 3 mm for the single jet configuration and 1.5 mm for the four jet configurations to keep the cross sectional area constant. Here the same holds as for the investigations on the flat plate. The generic missile configuration was mounted on a balance to measure global forces which were taken for the calculation of the amplification factors. The Reynolds number was $Re = 47 \cdot 10^6 / m$. It is not quite sure whether the boundary layer was turbulent or still laminar in the region of interaction, as firstly the round nose retards transition and secondly, the body was not tripped.

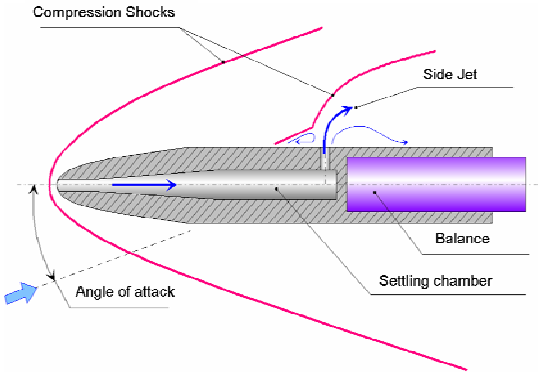

Figure 8: Schematic representation of the nose part of the missile configuration with the inlet through the front part of the nose providing the side jet.

3.2 Numerical simulation of the generic missile configuration

For the numerical calculation of the generic missile, grid set up and the procedure during the calculations the same holds as for the flat plate. The only differences result from the different model geometry and were realised accordingly. For the case of the full body configuration a stretching factor of 1.36 and a number of 22 layers for the resolution of the boundary layer were set in the initial grid. The jet pressure ratio p_{0jet}/p_∞ was set to 63, which differs by nearly a factor of 2 to the experiment. The side jet itself was modelled differently from the experiment. Whereas in the experiment the flow was directed through the nose of the model, the side jet was numerically realised by the same boundary condition of the supersonic inflow as on the flat plate. Hence, the friction and herewith drag that is generated also in this part of the physical model, is not calculated numerically. Consequently, the numerical and experimental results will differ from each other, but the tendencies of the efficiency of different jet configurations have to be the same and will be compared.

3.3 Results of the generic missile configuration

Based on the wind tunnel tests, the numerical cases chosen were the single jet for reference purposes, four jets side-by-side and in-line. The angle of attack of the numerical simulations was α = 0 and 10°. Oil flow visualisations were conducted on the full body configuration to gain an impression what the flow is like for different jet configurations on the test model. In Figure 9a-d the single jet case and the case of four jets side-by-side can be seen quantitatively. Due to the girthed area of the images of the numerical simulations, the images of the calculation and the experiment do not have exactly the same size and are distorted to each other, but they give an overview about the general flow features.

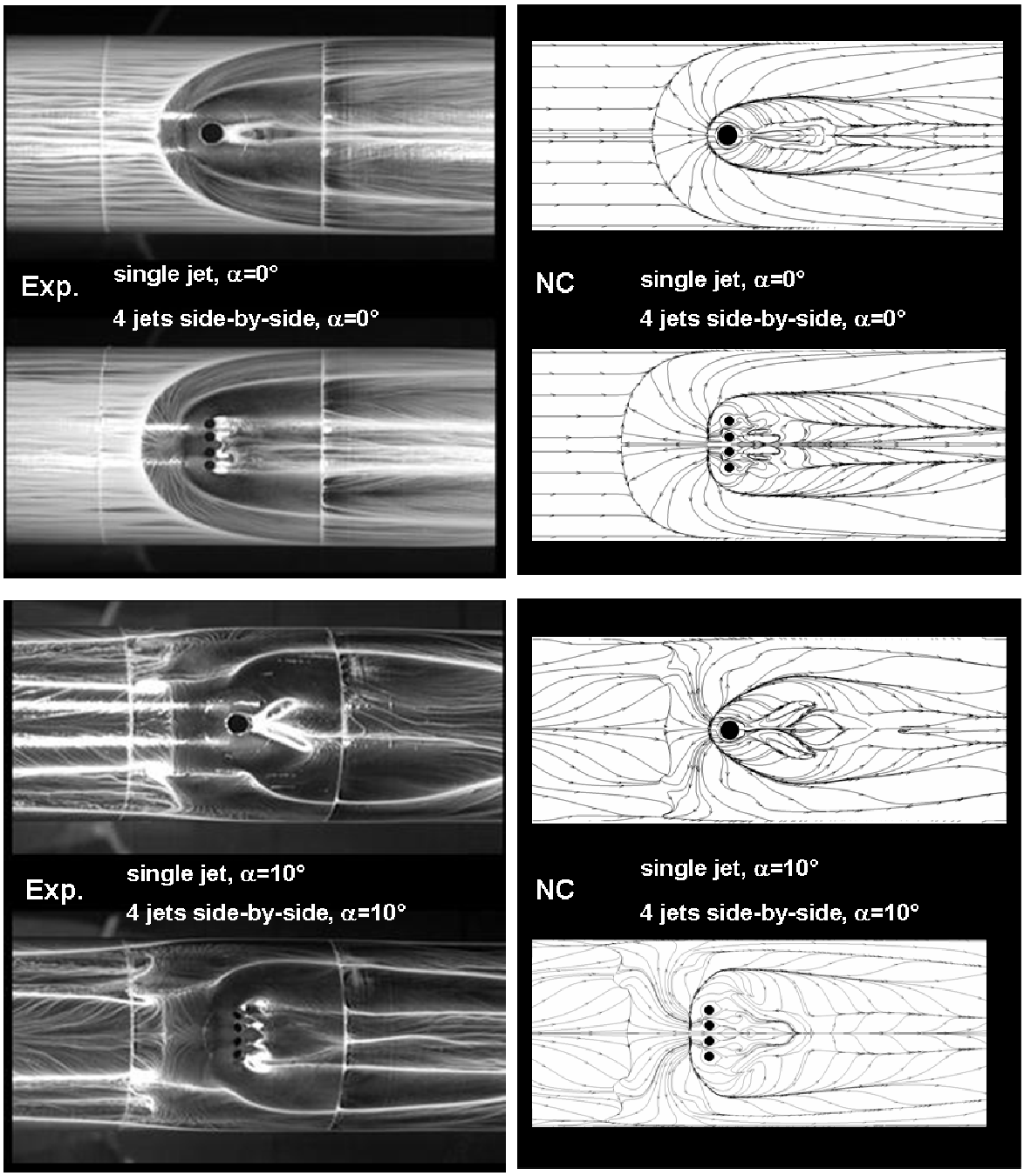

Figure 9a-d: Comparison of oil flow visualisations from the experiment (left hand side) and streamlines from the numerical calculations (right hand side). Top row: single jet, angle of attack 0°, 2nd row: 4 jets side-by-side, angle of attack 0°, 3rd row: single jet, angle of attack 10°, bottom row: 4 jets side-by-side, angle of attack 10°.

Figure 9a and b show the comparison of oil flow visualisation of the experiment and the numerical simulation of the single jet and the four jet side-by-side jet case for an angle of attack of $\alpha = 0°$. As the jet pressure ratio is not the same, the figures cannot be compared directly. The numerical jet pressure ratio is with 63 nearly twice as high as of the experiment ($p_{0jet}/p_{\infty} = 33$), so the separation zone has to be larger than for the experiment and this can be seen on the figures. The shape of the separation zones differs also between numerical simulation and experiment. Figure 9c and d show the same cases for an angle of attack

of $\alpha = 10°$. The blowing jet is interacting with the vortices that are developing on the body's lee-side. As far as can be seen from the images, is the separation zone in the experimental case not very much bigger than the upper half of the body which is shown on the image, and this remains for both shown cases as well as for both angles of attack. The numerical case shows a separation zone which is bigger than the half that can be seen and it stretches a little further down around the body.

Figure 10 shows the lift coefficient for the different test cases. The black line resembles the generic body without jet interaction as a reference. Due to the alignment of the nozzles on the body, the jet interaction provides a down-thrust which is indicated by the blue arrows. The largest effect comes from the case four jets side-by-side.

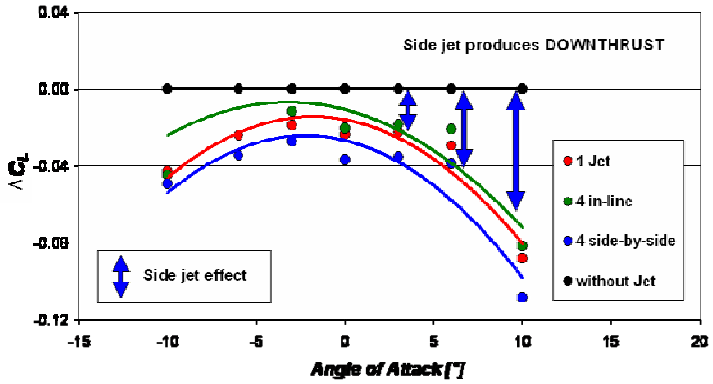

Figure 10: Diagram of different experimental jet configurations. All measurements are related to the case without an issuing jet.

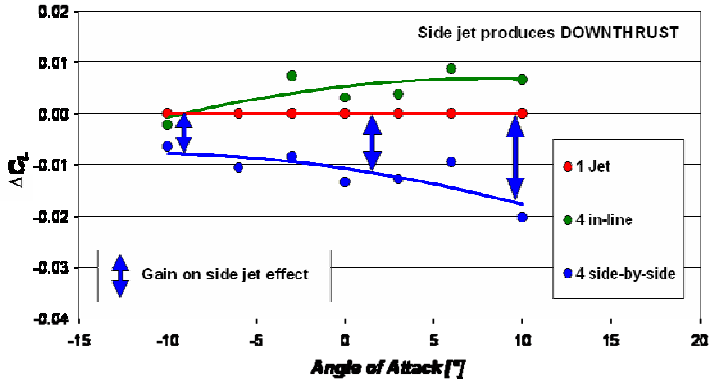

Figure 11: Down-thrust of jet interaction. All cases are related to the single jet case.

Figure 11 shows again the lift coefficient, but now in relation to the effect of the single jet. As the side jet produces a down-thrust, it can be seen from the positive values that the four jets in-line are less effective than the four jets side-by-side.

Amplification factors for full body configurations are usually lower than amplification factors measure on flat plates. This is confirmed also by this study. Compared with literature, different values were found for cylindrical missile configurations. [2] gained amplification factors of about 1 for round nozzles in a Mach number range between $2 < M < 10$. For another missile configuration, [4] found an alleviation of the jet effect, gained for a round nozzle with a diameter of 10 % of the cylindrical body of 40 mm diameter,

which is according to the experiments described here. K_F was determined with 0.19 - 0.41 for a Mach 3 flow and jet pressure ratios of $50 < p_{0jet}/p_\infty < 97$. [8] gained amplification factors of $0.95 < K_F < 1.15$ for a body of revolution with a round nozzle in a supersonic flow between $2.43 < M < 3.9$.

Figure 12 displays the gain that results from the different test cases in terms of the total amplification factor which were gained from the force measurements in the wind tunnel. The curves drawn connecting the points are no real fits but just meant to get the idea of the distribution of the points for the three cases. Here it becomes clear that the four jets side-by-side is a favourable configuration as in relation to the single jet it can be seen that the four jets in-line are less effective than also the single jet which was the reference case.

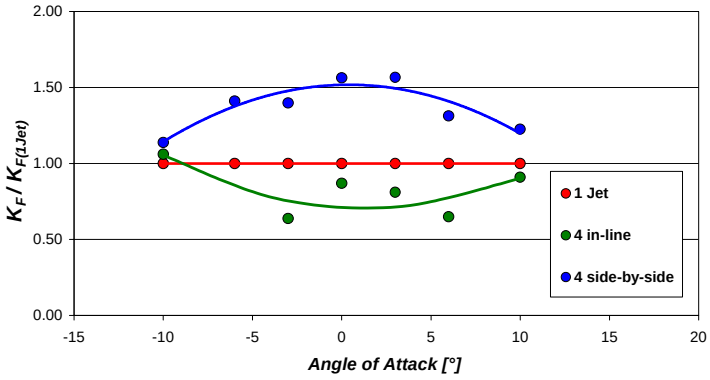

Figure 12: Diagram of the jet interaction for the different test cases. All cases are related to the case of the single jet to see the different effect in comparison to the reference case.

Figure 13 shows the amplification factor in flow direction K_{FX} of the generic missile of the numerical calculation at an angle of attack of $\alpha = 0°$, gained with the same procedure as the flat plate data. Also for the generic configuration the numerical amplification factor changes along the length of the body. The different shapes and sizes of the separation zones are also here causing different amplification factors with a ceasing difference towards the end of the body at 133 mm.

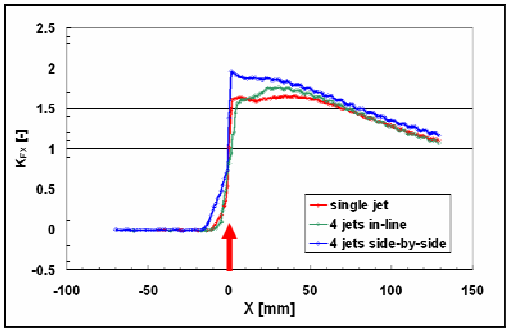

Figure 13: Distribution of the amplification factor K_{FX} in comparison for the three different cases on the full body configuration.

In contrast to the flat plate, the amplification factor does not approach an asymptotic value, as at the end of the body K_{FX} is still changing. This is due to the fact that the flow is moving circumferentially away from the body, distributing the effect side- and downwards of the body. Here, several effects have to be taken into account: As said before, the nose part of the generic missile was modelled differently for experiment and simulation resulting in an additional force for the experiment, which cannot be captured by the

simulation. Secondly, the jet pressure ratio was not the same for the numerical calculation as for the experiment. The numerical jet pressure ratio is with 63 nearly a factor 2 higher than the jet pressure ratio for the experiment. The amplification factors are herewith not directly comparable but they are consistent with the finding of [7] that the amplification factor decreases with increasing jet pressure ratio as K_{FX} is considerably lower for the numerical calculations. Also the tendency of the more favourable configuration of the 4 jets side-by-side is also given by the numerical simulation.

However, distinct differences can be seen between numerics and experiment, which are not totally understood yet. So are the experimental amplification factors much larger and the differences between the different configurations are much more pronounced than it is apparent in the numerical calculations. Differences do occur due to the fully turbulent calculation whereas in the wind tunnel laminar turbulent transition takes place somewhere on the forebody of the model. For clarification it would be reasonable to repeat the experiment and numerical calculations at laminar conditions at reduced Reynolds-numbers or at turbulent conditions with a tripped boundary layer to have the same conditions in this important respect.

4.0 CONCLUSIONS

A major investigation was conducted with the target to gain a deeper understanding of the flow phenomena produced by the interaction of a side jet issuing into a supersonic flow and to find a configuration which is more favourable and stable in a broad range of angles of attack. For this purpose, oil flow visualisations, surface pressure measurements and numerical simulations were performed on a flat plate, as here the effects become clearer and are easier to measure and to evaluate. A main focus of the evaluation was put on the total amplification factor K_F and the amplification factor in flow direction K_{FX}, which is a direct measure for the efficiency of the side jet control. While the results for the flat plate fit well into the range of available literature, the analysis of the numerical data revealed an aspect that is in contrast to the former opinion. While it was assumed that in the wake of the jet a low pressure region exists that is big enough to compensate the high pressure area and herewith reduces the amplification factor, it could be shown that the low pressure region is in fact only very small and easily been “eaten up” by the surrounding high pressure. Hence, the amplification along the flat plate is positive as soon as the flow separates and finally reaches an asymptotic value that does not change anymore towards the end of the flat plate. The difference in the amplification factor for the three tested configurations is only very small and only visible in the vicinity of the nozzles. The investigation on the generic configuration showed different results for the numerical and the experimental amplification factors. While larger differences occur for the different configurations in the experiment, the numerical calculations predict similar values at the end of the body and show differences between the three configurations only in the vicinity of the nozzle, which is a similar behaviour to the flat plate. This finding also has an influence on the exact position of a side jet control nozzle along a missile. So it may be more favourable to mount the jet nozzles towards the tail of the body. This is a request that was mentioned before, but for the wrong reasons. So far, it was wanted to mount the nozzle at the rear of the body to be able to cut off a large low pressure region. As the low pressure region is not as pronounced as always thought, it is not necessary to do so. It may be more favourable to mount the nozzle towards the rear of the body to have the greatest gain from the amplification and also from the effect of different configurations which increasingly equalise with increasing distance from the nozzle. For a final assessment of the position of the nozzle, it has to be kept in mind that also the pressure ratio plays an important role.

From the experimental studies followed that the most favourable investigated configuration consisted of 4 jets mounted side-by-side as here the positive effect remained very stable over the investigated angles of attack ranging from $-10° < \alpha < 10°$. The numerical results indicate that the exploitation of this gain is a question of the position of the nozzles. However, the size of the amplification factor of the numerical full body configuration deviates substantially from the experimental results, where it is not clear now, what causes this difference.

REFERENCES

[1] Amick, JL, Hays, PB (1960): Interaction effects of side jets issuing from flat plates and cylinders aligned with a supersonic stream, WADD-TR-60-329

[2] Brandeis, J, Gill, J (1996): Experimental Investigation of Side-Jet Steering for Supersonic and Hypersonic Missiles, Journal of Spacecraft and Rockets, Vol. 33, No 3, pp 346-352

[3] Gerhold, T, Evans, J (1999): Efficient Computation of 3D-Flows for Complex Configurations with the DLR TAU-Code Using Automatic Adaptation, Notes on Numerical Fluid Mechanics, Vol.72, Vieweg.

[4] Gnemmi, P, Schäfer, HJ (2005): Experimental and Numerical Investigations of a Transverse Jet Interaction on a Missile Body, for 43rd AIAA Aerospace Sciences Meeting and Exhibit, Reno/NV, USA, January 10-13, 2005, Internal Report of ISL, PU 603/2005

[5] Kovar, A, Schülein, E (2006): Comparison of Experimental and Numerical Investigations on Side Jets in a Supersonic Cross Flow, accepted for publication in The Aeronautical Journal.

[6] Ludwieg, H, Hottner, Th, Grauer-Carstensen, H (1970): Der Rohrwindkanal der Aerodynamischen Versuchsanstalt Göttingen, Jahrbuch der DGLR 1969, S. 52 – 58

[7] Maurer, F (1966): Three-Dimensional Effects in Shock-Seperated Flow Regions Ahead of Lateral Control-Jets Issuing from Slot Nozzles of Finite Length, AGARD-CP-4, Part 2, Flow Separation, pp 605-634

[8] Naumann, KW, Srulijes, J (1985): Die Flugbahnsteuerung mittels seitlich austretender Strahlen. Literaturübersicht, Bericht aus dem ISL, R 117/85

[9] Naumann, KW, Ende, H, Mathieu, G, George, A (1993): Experiments on interaction force of jets in hypervelocity cross-flow in a shock tunnel, AGARD-CP-534, Computational and Experimental Assessment of Jets in Cross Flow, Symp. in Winchester, UK, 19th-22nd April, 1993

[10] Schülein, E, Zheltovodov, A (2001): Documentation of Experimental Data for Hypersonic 3-D Shock Waves/Turbulent Boundary Layer Interaction Flows, Internal Report IB 223-99 A 26, DLR, Göttingen, Germany

[11] Schwamborn, D, Gerhold, T, Hannemann, V (1999): On the Validation of the DLR TAU-Code, Notes on Numerical Fluid Mechanics, Vol.72, Vieweg

[12] Spaid, FW, Zukoski, EE (1968): A Study of the Interaction of Gaseous Jets from Transverse Slots with Supersonic External Flows, AIAA Journal, Vol 6, No 2, pp 205-212, 1968

SYMPOSIA DISCUSSION – PAPER NO: 37

Discusser's Name: Dr K Naumann

Question:
Do you also plan to study supersonic thrusters?

Author's Name: Dr P Gnemmi

Author's Response:
In fact, the Mach number at the jet exit is already about 1.2. We can increase the velocity at the jet exit but it is not planned.

This page has been deliberately left blank

Page intentionnellement blanche

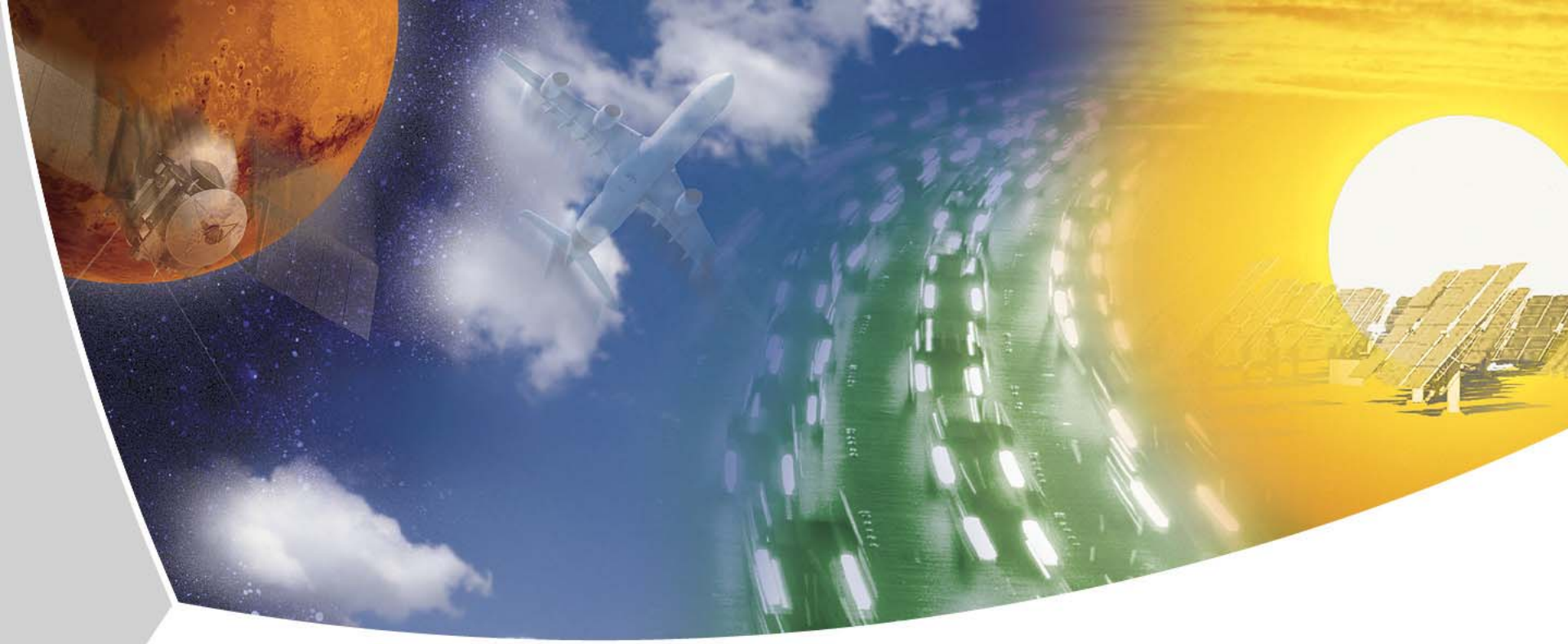

Effects of side jets in a supersonic flow – measured and calculated on a flat plate and a generic missile configuration

Anke Kovar, Erich Schülein – German Aerospace Center DLR

Deutsches Zentrum
für Luft- und Raumfahrt e.V.
in der Helmholtz-Gemeinschaft

Outline

- Description of Side Jet Control (SJC)
- Advantages / disadvantages
- Test conditions and results for the flat plate
- Test conditions and results for the generic configuration
- Conclusions

Description of side jet control

- **A jet is issuing under high pressure perpendicularly to the flow from the surface**
- **The jet force is used to control the missile**

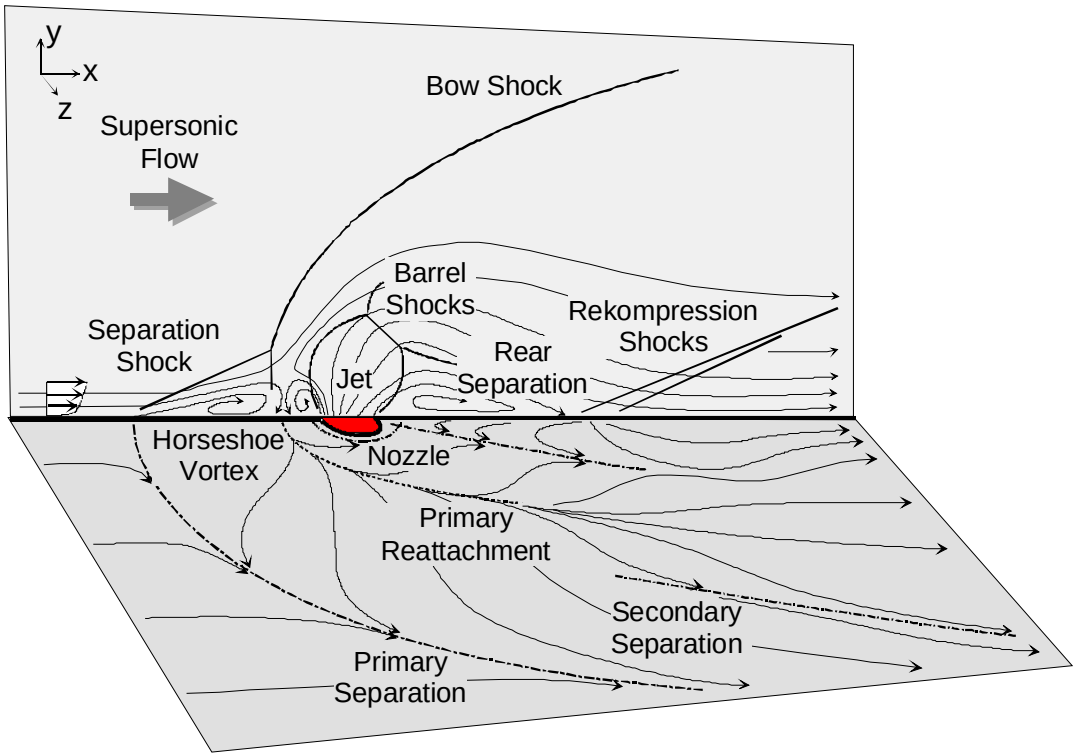

Advantages / disadvantages

Advantages	Disadvantages
Quick response (ms)	Interaction is difficult to predict
Applicability at low stagnation pressures (starting phase, large altitude)	Strong dependence on flight parameters (stagnation pressure)

Aim

- **Finding of a favourable configuration by experiments in the Ludwieg tube facility (RWG) and numerical calculations with the DLR-internally developed TAU-code**
- **Stable effect for a greater range of angles of attack**
- **Exploitation of interaction ?**
- **Special Interest: Amplification Factor $K_F = (F_j + F_i)/ F_j$**
- **To predict the effect using the DLR-TAU-code**
- **Usage of experimental and numerical data for validation**

Test conditions of flat plate

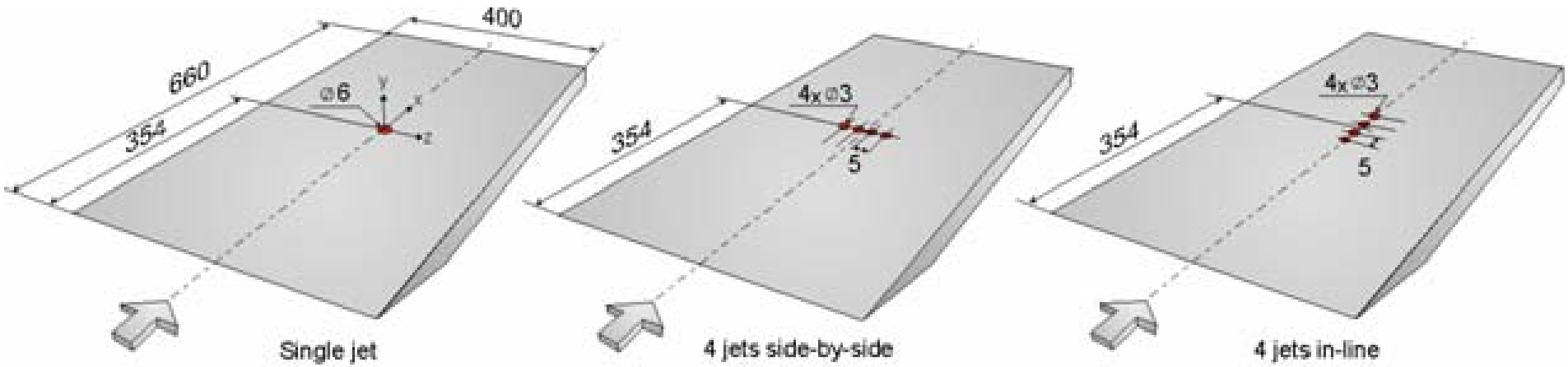

	Experimental	Numerical
Ma-No.	5	5
p_{oj}/p_{∞}	100	100
Re-No.	13 x 10^6	13 x 10^6
BL	turbulent at interaction	turbulent
Model	physical	Spalart-Almaras 1-Eqn

Results of flat plate - comparison

- surface pressure

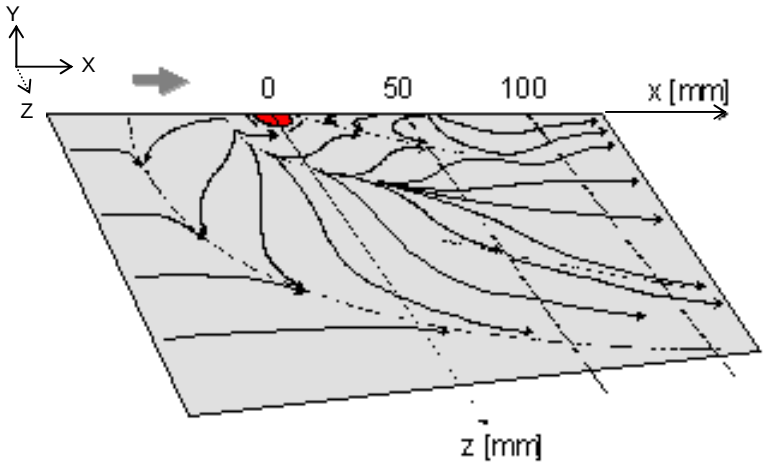

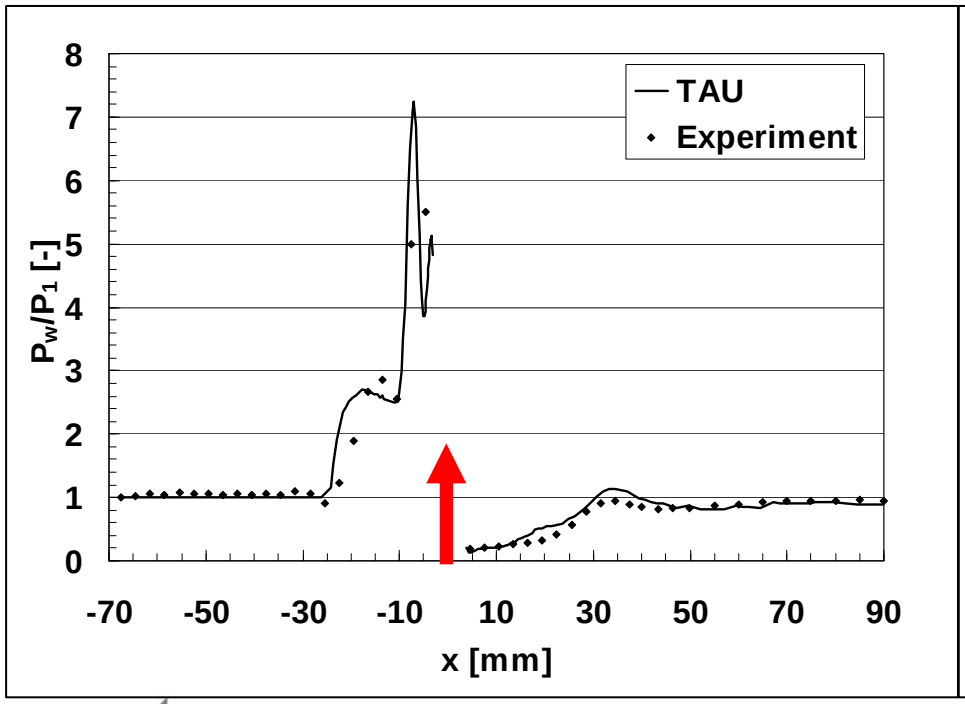

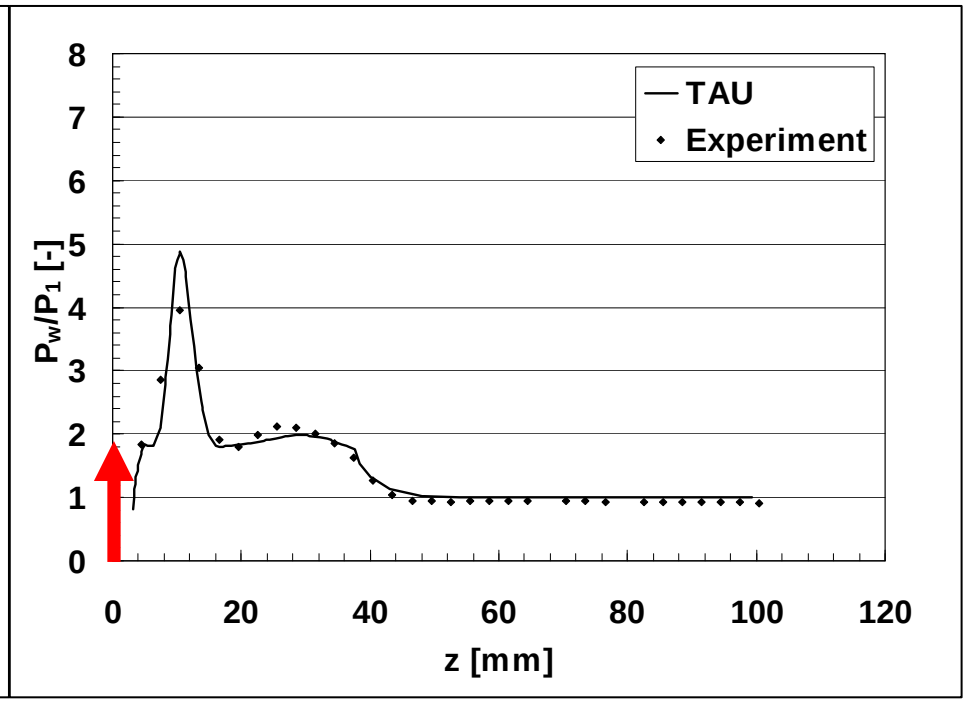

Results of flat plate - comparison
- wall streamlines

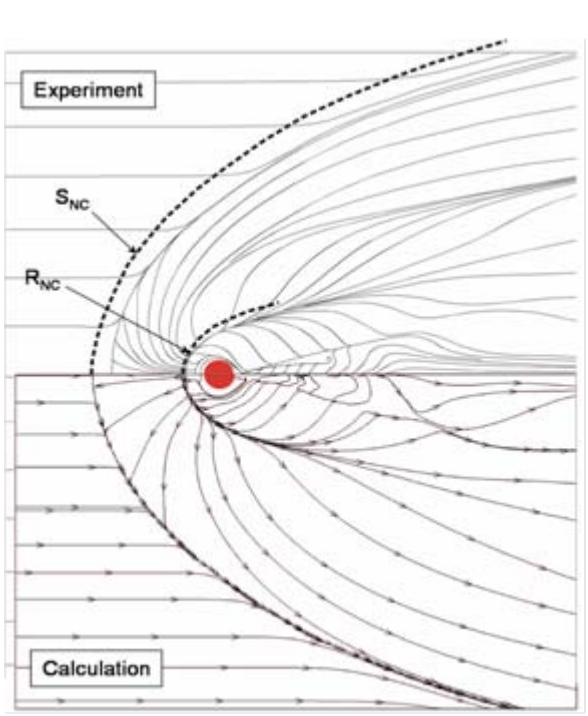

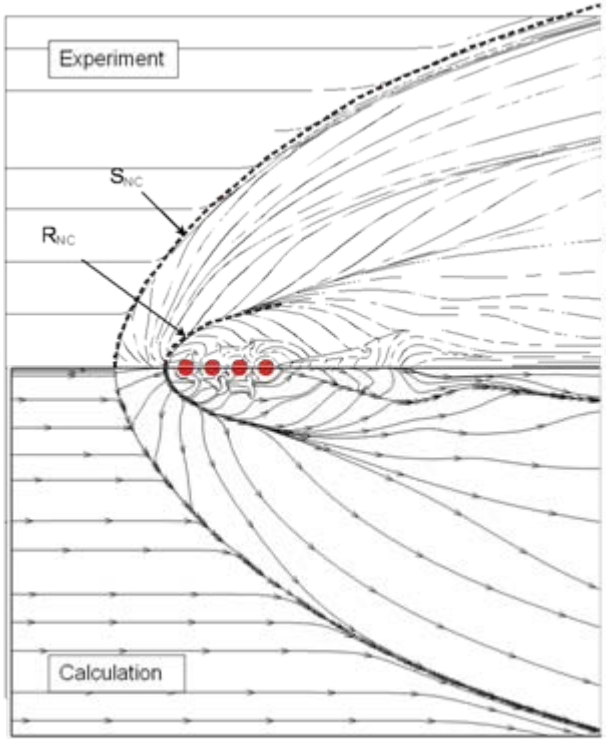

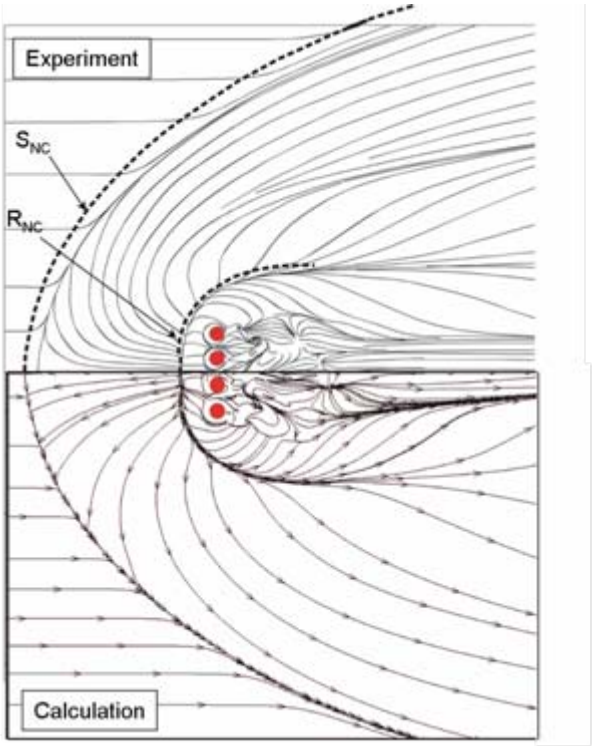

Numerical results of flat plate
- pressure difference

- **Pressure corrected with flat plate w/o jet**
- **Area of Δp < 0 is only very small**
- **Low pressure area in the wake cannot compensate high pressure area**

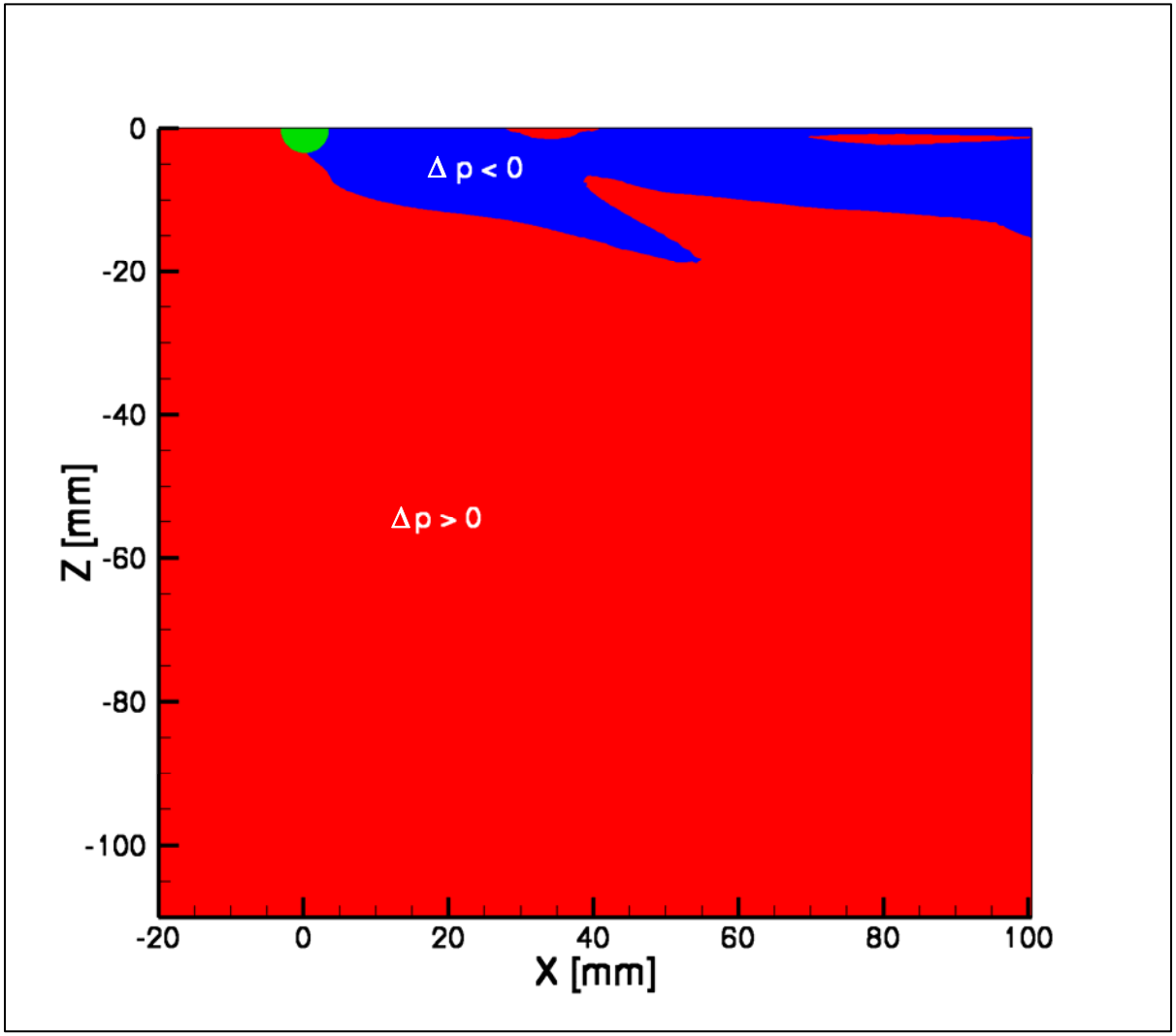

Numerical results of flat plate
- amplification factor

$$K_F = \frac{(F_j + F_i)}{F_j} \quad \rightarrow \quad K_{FX} = \int_{-x}^{x} \left(\int_{-z}^{z} \Delta p dz \right) dx$$

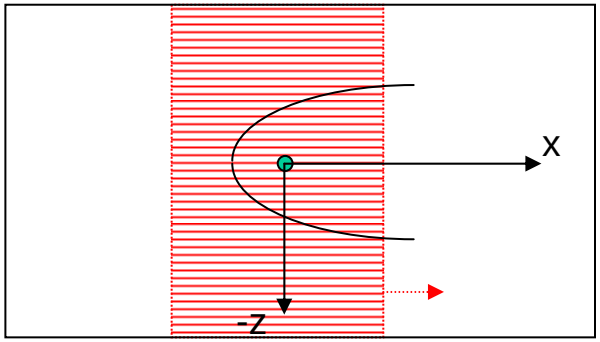

- No reduction in wake of jet
- Amplification Factor K_{FX} differs only in vicinity of jet position
- K_{FX} reaches asymptotic value

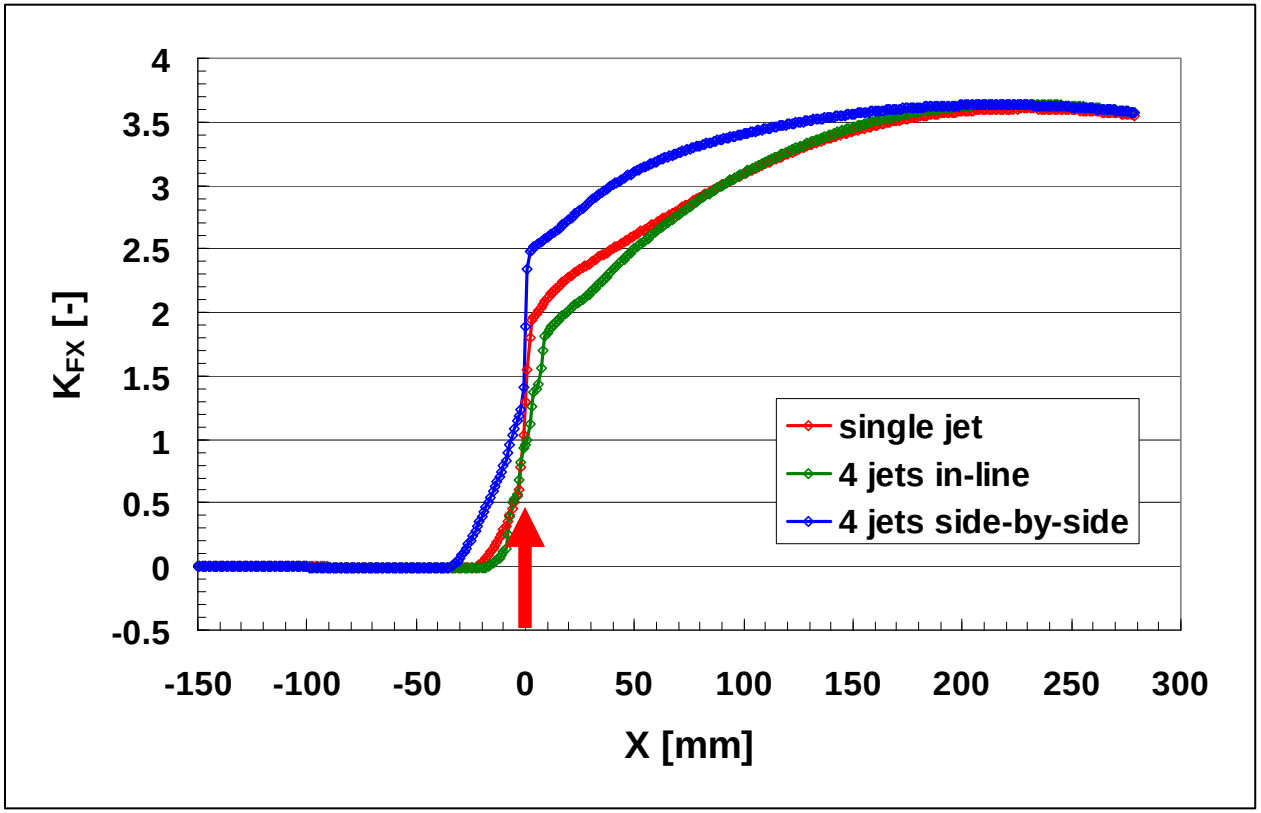

Summary of flat plate results

- Deviation in size of separation zone between Exp and TAU
- Differences are also related to interaction between indivdual jets

Numerical results show

- No reduction of K_{FX} in wake of jet!
- Amplification factor K_{FX} reaches asymptotic value for all three cases
- Differences in K_{FX} occur only in vicinity of jet position → important for jet positioning

Test conditions of generic missile configuration

	Experimental	Numerical
Ma-No.	5	5
p_{oj}/p_{∞}	33	62
Re-No.	47 x 10^6	47 x 10^6
BL	not sure	turbulent
Jet source	flow through nose	circular area set as outflow cond.

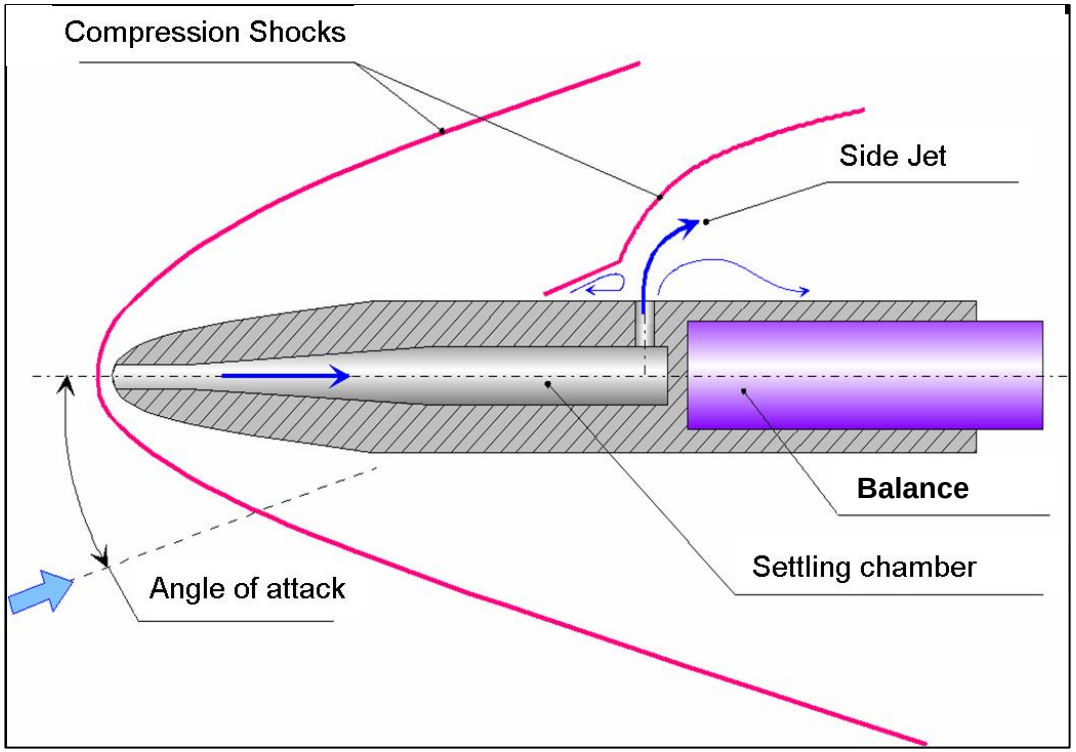

Experimental results of generic missile configuration

- Side jet produces downthrust indicated by blue arrows

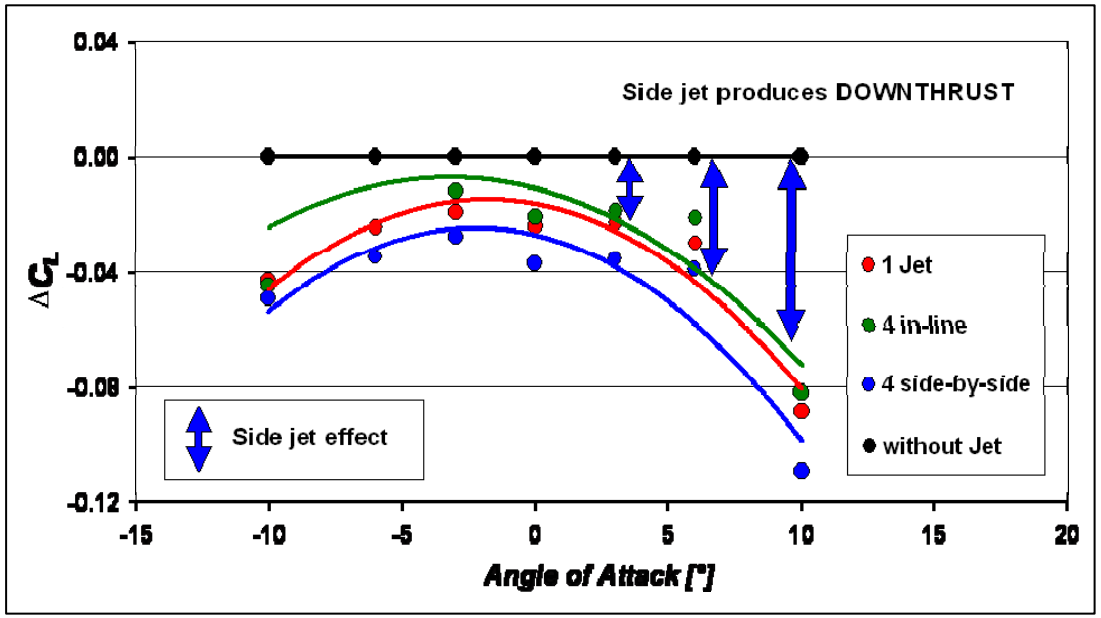

- Gain larger for four jets side-by-side than in-line

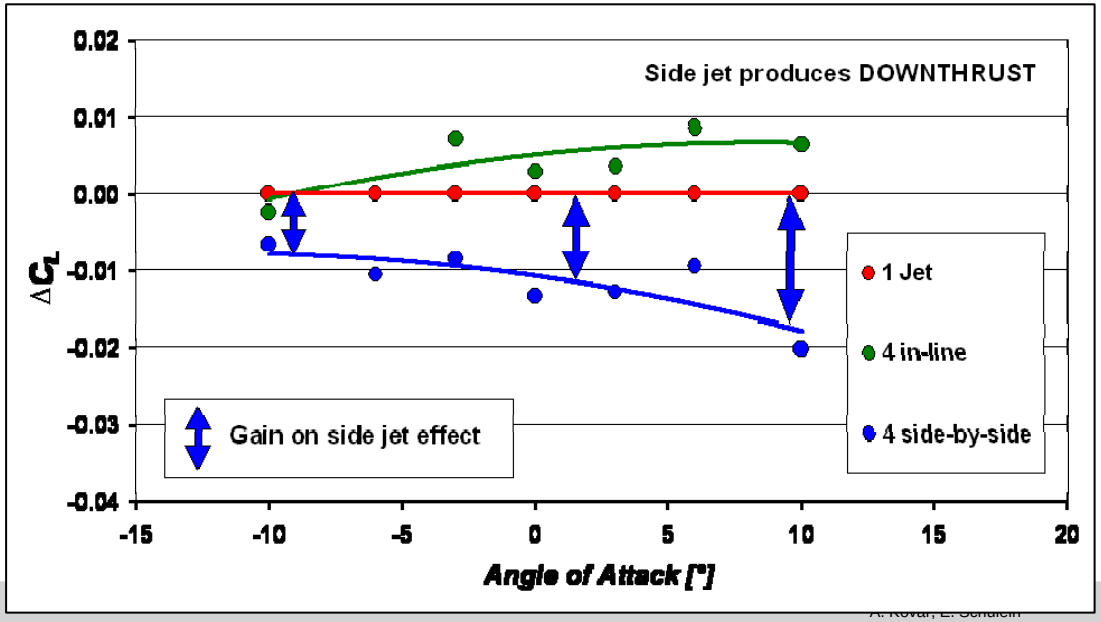

Experimental results of generic missile configuration

- **Four jets side-by-side is more favourable over whole range of α !**

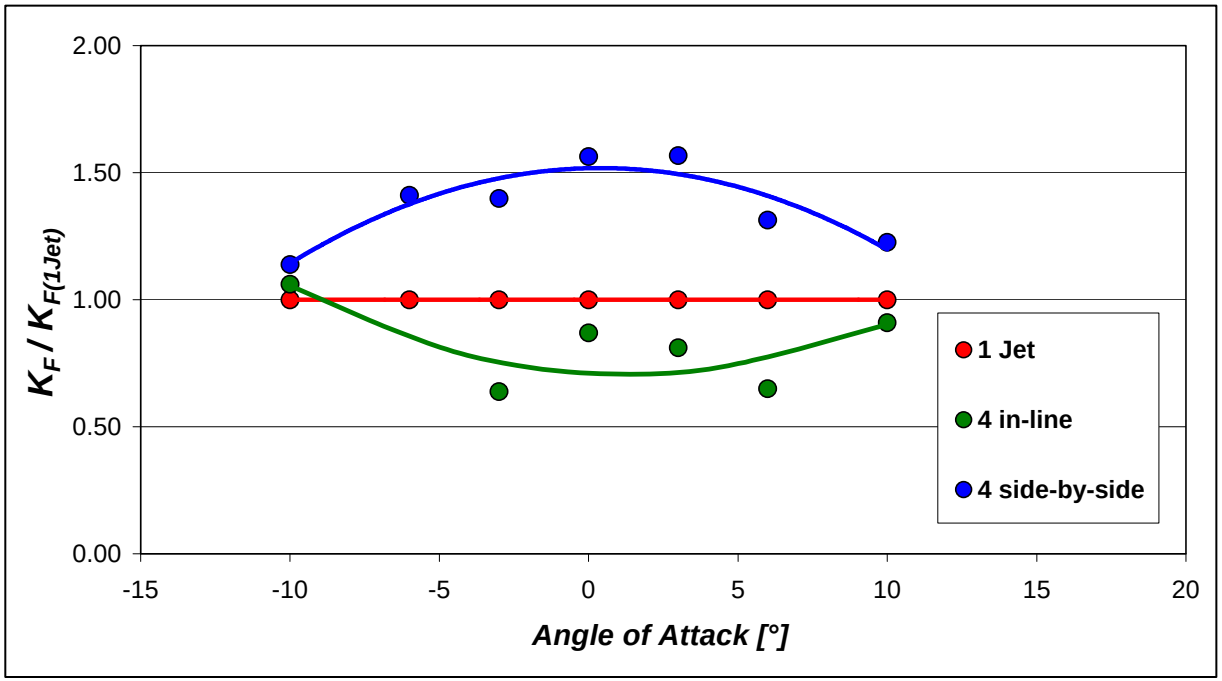

Numerical results of generic missile configuration
- amplification factor at α=0°

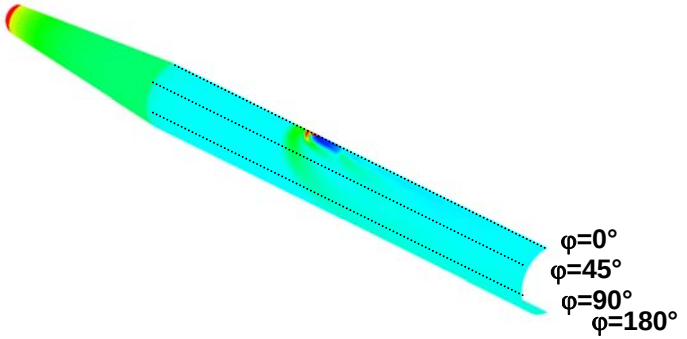

- **Amplification Factor K_{FX} differs only in vicinity of jet position**
- **K_{FX} is decreasing over the body as the high pressure flow moves circumferentially away from the jet**

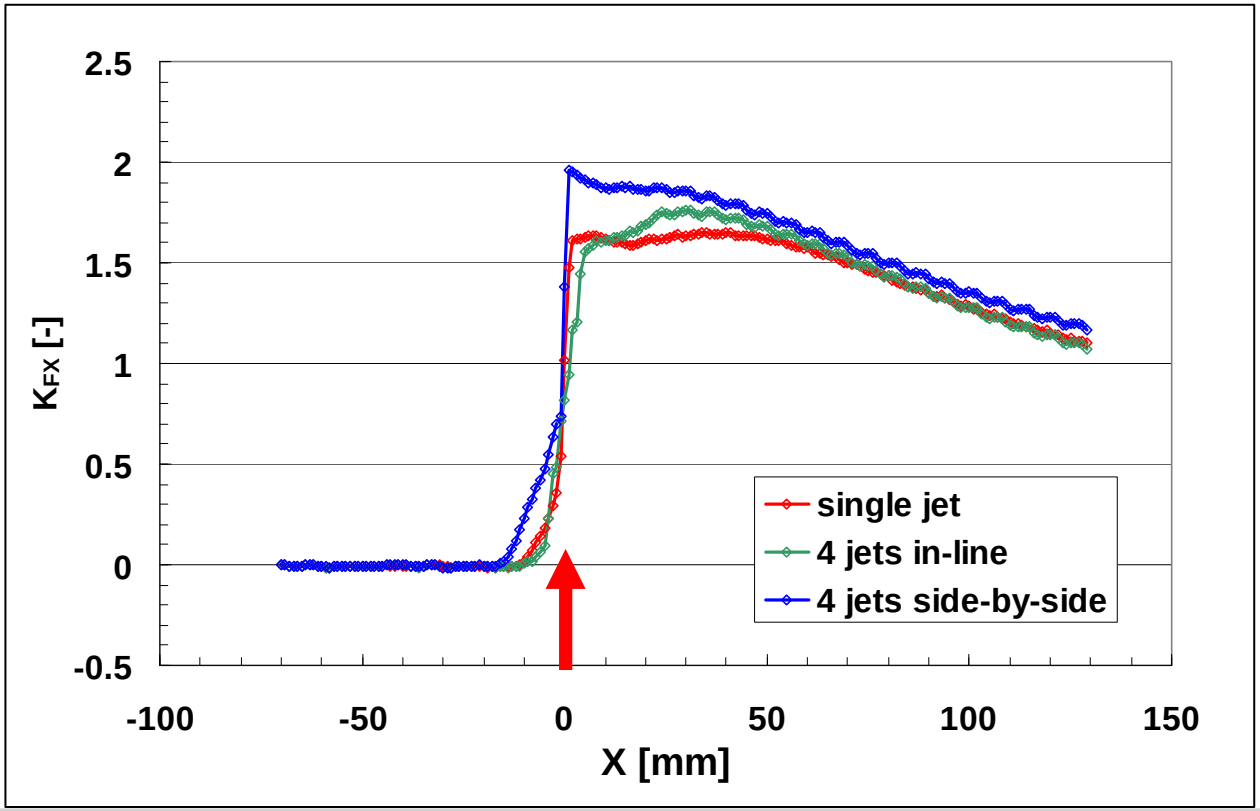

Summary of generic missile results

- Direct comparison between Experiment and TAU impossible due to different p_{oj}/p_{∞}
- Tendencies in jet efficiency is similar between experiment and TAU
- Most favourable configuration of all is four jets side-by-side
- Experiment shows distinct differences in K_F whereas TAU does not

Conclusions

	Experimental	Numerical
Most favourable configuration	- four jets side-by-side (whole range of α)	- four jets side-by-side (α=0°)
Analysis of K_{FX} and K_F	-distinct differences for different configurations - larger values for experiment than for TAU	-asymptotic value for all configurations - no reduction in the wake
Simulation of main flow features (surface pressure and wall streamlines)		- main flow features were captured - small deviations in size of separation zone -according shift of separation lines